CHEMMEDCHEM

CHEMISTRY ENABLING DRUG DISCOVERY

Accepted Article

Title: Gold(I)-coumarin-caffeine-based complexes as new potential anti-inflammatory and anticancer trackable agents

Authors: Audrey Trommenschlager, Florian Chotard, Benoît Bertrand, Souheila Amor, Philippe Richard, Ali Bettaïeb, Catherine Paul, jean-Louis Connat, Pierre Le Gendre, and Ewen Bodio

To be cited as: *ChemMedChem* 10.1002/cmdc.201800474

Link to VoR: http://dx.doi.org/10.1002/cmdc.201800474

A Journal of

ChemPubSoc Europe

WILEY-VCH

www.chemmedchem.org

WILEY-VCH

FULL PAPER

Gold(I)-coumarin-caffeine-based complexes as new potential anti-inflammatory and anticancer trackable agents

Audrey Trommenschlager,[a] Florian Chotard,[a] Benoît Bertrand,[a] Souheila Amor,[a] Philippe Richard,[a] Ali Bettaïeb,[b,c] Catherine Paul,[b,c] Jean-Louis Connat,[d] Pierre Le Gendre,[a] and Ewen Bodio*[a]

[a] A. Trommenschlager, Dr F. Chotard, Dr B. Bertrand, Dr S. Amor, Dr P. Richard, Prof. P. Le Gendre, and Dr E. Bodio
ICMUB UMR6302, CNRS
Univ. Bourgogne Franche-Comté
F-21000 Dijon, France.
E-mail: ewen.bodio@u-bourgogne.fr
[b] Prof. A. Bettaïeb, and Dr C. Paul
EPHE, PSL Research University,
75000, Paris, France
[c] Prof. A. Bettaïeb, and Dr C. Paul
LIIC, EA7269
Université de Bourgogne Franche Comté
21000, Dijon, France
[d] Prof. J.-L. Connat
Biologie Animale Cellulaire et Moléculaire
Univ. Bourgogne Franche-Comté
6 Bvd Gabriel, F-21000 Dijon, France

Supporting information for this article is given via a link at the end of the document.((Please delete this text if not appropriate))

Abstract: Three new gold(I)-coumarin-based trackable therapeutic complexes and two non-trackable analogues have been synthesized and fully characterized. They all display antiproliferative properties on several types of cancer cell lines including colon, breast, and prostate. Two complexes displayed significant anti-inflammatory effect, while one displayed a pro-inflammatory behaviour – highlighting the impact of the position of the fluorophore on the caffeine scaffold. Additionnally, the three coumarin derivatives could be vizualized *in vitro* by two-photons microscopy.

Introduction

The interest for gold salts in medicine dates back to Chinese Antiquity. Nowadays, their main use in clinics concerns the treatment of rheumatoid arthritis with respect to their anti-inflammatory properties.[1] [(2,3,4,6-tetra-*O*-acetyl-1-(thio-κS)-β-d-glucopyranosato)(triethyl-phosphane) gold(I)] – also known as auranofin (or Ridaura®) – is one of the most studied gold complexes (Figure 1).

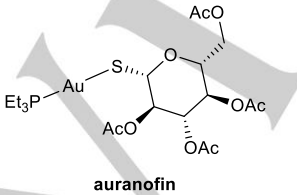

auranofin

Figure 1: Structure of auranofin.

Different researchers reported on its properties to fight cancer, HIV/AIDS, parasitic and bacterial infections...[2–4] The recent NIH's campaign for finding new applications for "old drugs" has led to the entrance of auranofin in four clinical trials for the treatment of some cancers as well as one clinical trial where auranofin is used to decrease the pain of patients with paclitaxel-induced pain syndrome (paclitaxel is an anticancer drug).[5] This highlights the potential of gold derivatives as a treatment combining anticancer and anti-inflammatory actions.

It is now admitted that inflammation is a critical component of tumour initiation and progression. Indeed, the tumour microenvironment, which is largely orchestrated by inflammatory cells, is an indispensable participant in the carcinogenesis process, fostering proliferation, survival and migration,[6] hence our interest in building products to target the proliferation of cancer cells and their inflammatory microenvironment. In the last few years, Trávníček and coll. designed several adenine-based gold complexes, which displayed anticancer and anti-inflammatory properties.[7–10] Very recently, we have drawn our inspiration from their work and combine it with our expertise in the design of trackable metal-based therapeutics (a kind of optical theranostics[11]) to synthesize a fluorescent gold(I)-homobimetallic complex **A**, which gave very promising results.[12]

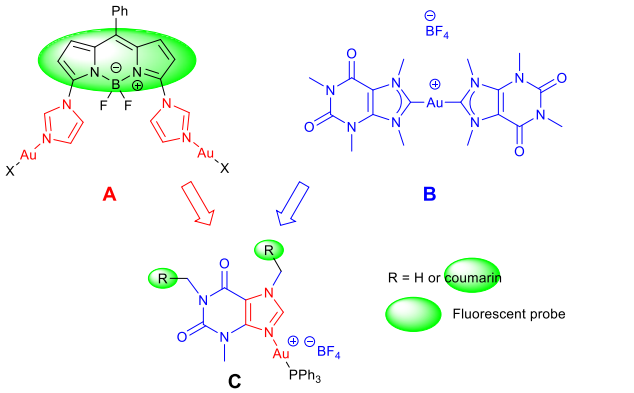

Scheme 1: Strategy developed in this paper combining results of two of our previous studies.[12,13]

Otherwise, we have developed numerous Au(I)-*N*-Heterocycle-Carbene-based anticancer agents.[14,15,13,16,17] Among the structures investigated, we noticed that replacing imidazolium or benzimidazolium scaffold by a caffeinium derivative can increase dramatically the biological suitability of the corresponding complex **B** (decrease of the toxicity on healthy tissues) (Scheme 1).[13,18] We thought it would be interesting to see if the same behaviour can be observed when caffeine derivatives are used as "L-type" *κ*N-ligand. Thus, we decided to design trackable caffeine-based Au(I)-complexes. BODIPYs are among the best fluorophores for tracking therapeutics.[19] However their high lipophilicity is not well suited for imaging poorly water soluble molecules such as caffeine derivatives. Consequently, we moved to coumarin, which also gave us very good results in the past (we developed a highly fluorescent family of coumarin-based gold(I) complexes, which display interesting antiproliferative properties on several cancer cell lines and, moreover, one of them displays very low toxicity on both zebrafish larvae and mice).[16,20,21] Moreover, several studies reported on the anti-inflammatory effect of coumarin derivatives.[22–25] Thus, coumarin moiety may be more than just a fluorescent probe. Convinced of the high potential of this approach, we designed a family of gold complexes to investigate the impact on their biological properties of the caffeine *vs* benzimidazole scaffold, of the presence of the coumarin probe, and of its position on caffeine scaffold (Scheme 1).

Here we report the synthesis, the characterization, and the biological evaluation of five new gold(I) complexes and their corresponding ligands. The Au(I) complexes demonstrated interesting cytotoxic properties against different human cancer cell lines. However, surprisingly, the impact of the ligands on anti-proliferative effect appeared to be very low, while it was dramatic on their anti-inflammatory properties. Taking advantage of the coumarin dye, the uptake of the compounds was observed by two-photon microscopy.

Results and Discussion

Synthesis

The coumarin ligands **1**-**3** were prepared by direct alkylation of their commercially available precursors with the 4-bromomethyl-7-methoxycoumarin. As expected, selective monoalkylation occurred on the "NH" position (**Erreur ! Référence non valide pour un signet.**).

Ligands **1**, **2**,[26] **3**, and their methyl analogues – *N*-methylbenzimidazole and caffeine – were reacted with $Au(PPh_3)Cl$ in the presence of the chloride abstractor $AgBF_4$ to convert them to the corresponding gold(I) complexes **4-8** (**Erreur ! Référence non valide pour un signet.**). The formation of the complexes can be easily monitored by ^{31}P-NMR. Moreover, on ^{1}H-NMR spectrum, it is interesting to note that the imidazole "C-H" proton shifted from around 7.6 ppm to around 8.9 ppm, which is close to the chemical shift observed for caffeinium derivative. This highlights the imidazolium character of the complexes.

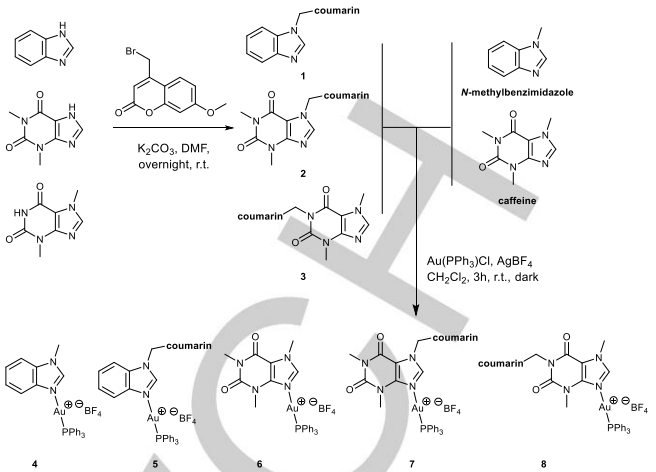

Scheme 2: Syntheses of gold(I) complexes **4**-**8**.

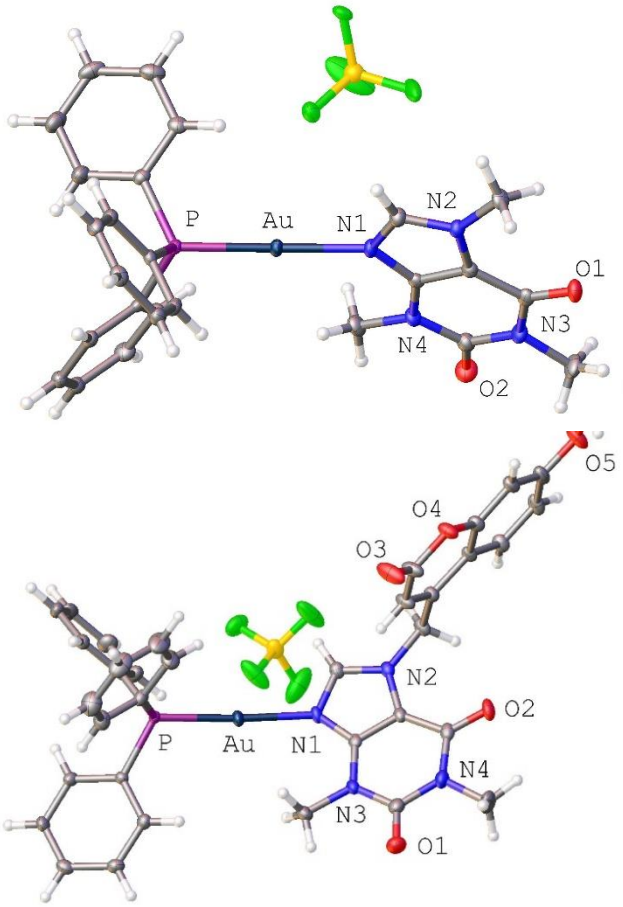

Figure 2: Ortep views of **6** (up) and **7** (down). For clarity the BF_4^- disorder for **6** and the diethyl ether solvate molecule for **7** are not shown.

The different compounds have been fully characterized by usual analytical techniques. Monocristals of **6** and **7** suitable for X-ray diffraction have been obtained by diffusion of diethyl ether in a dichloromethane solution of the complexes (Figure 2). The structures display the usual linear coordination

scheme of Au(I) ion (N-Au-P: 175.56(7)/176.16(8)° respectively) and the non-coplanarity of coumarin bicycle and theophiline one (dihedral angle: 82.50(8)° between mean planes) (Figure 2).

"N-Au" and "P-Au" bond lengths of the two complexes are very similar (N-Au: 2.075(2)/2.095(3)Å and P-Au: 2.2358(7)/ 2.2302(8)Å respectively) and are in the range of the ones reported for a benzimidazole analogue, which highlights the innocent character of the imidazole ring substituent – methyl or methylcoumarin – and of the nature of the second ring on the strength of the gold(I) complex moiety. Moreover, a comparison with the numerous X-ray structures of phosphine gold cationic complexes ([P-Au-P]$^+$) reported in the CCDC database highlights the fact that, in our complexes, the "P-Au" bond is shorter (2.23Å *vs.* ≈ 2.31Å for [P-Au-P]$^+$ complexes).

Photophysical characterization

The photophysical properties of the three coumarin-gold(I) complexes **5**, **7**, and **8**, as well as their corresponding ligands **1**, **2**, and **3** were measured in DMSO (Table 1).

Table 1: Photophysical data of the compounds **1**, **2**, **3**, **5**, **7**, and **8** in DMSO at 293K.

Compound	λ_{abs} (nm)	λ_{em} (nm)[a]	ε ($M^{-1}.cm^{-1}$)	Φ_f (%)[b]
1	320	393	16,000	18
2	320	392	13,000	2
3	319	390	16,000	18
5	322	393	15,000	34
7	322	397	16,000	5
8	320	392	14,000	22

[a]: λ_{ex} = 325 nm
[b]: 9,10-diphenylanthracene (Φ_f = 0.90, λ_{exc} = 325, in cyclohexane).[27]

As expected, the methylene group between the coumarin and the heterocycle prevents any conjugation extension phenomenon, which results in the same characteristic wavelengths for all the ligands: a maximum absorption wavelength around 320 nm and an emission one around 395 nm. For the same reason, the coordination of gold(I) atom does not induce any significant red or blue shift.

On the contrary, quantum yields of fluorescence of the different compounds are not similar. In particular, ligand **2** and its corresponding complex **7** display poor quantum yields. It is difficult to rationalize the observed differences. Indeed, it could be suggested that caffeine may induce a quench of the fluorescence but compounds **3** and **8** display satisfying quantum yields. Another explanation could be that the proximity of the coumarin to the imidazole ring may cause a photoinduced electron transfer phenomenon but ligand **1** displays an interesting quantum yield. Otherwise, it is worth noting that, as it was observed in previous studies,[12,28,29] the coordination to gold(I) ion does not quench the fluorescence, it even increases the quantum yield of **1** and **2** by a factor two.

Evaluation of antiproliferative properties

The antiproliferative properties of *N*-methylbenzimidazole, caffeine, of the ligands **1**-**3**, and of the gold(I)-complexes **4**-**8** were evaluated on breast (MDA-MB-231), prostate (PC3), and colon (SW480) human cancer cell lines and on a human non-cancerous cell line (HEK293T) in comparison to auranofin (Table 2). None of the ligands displays a significant cytotoxicity (IC_{50} ≥ 75 µM), while all the complexes displayed a significant cytotoxicity (IC_{50} ≈ 15 µM) on the cancer cell lines. Their activity is slightly lower than auranofin and in the range or higher than some clinically used anticancer agents that we have tested on SW480 such as etoposide (IC_{50} = 16 µM) and 5-fluorouracil (IC_{50} = 26 µM). It is worth noting that the introduction of the coumarin probe did not lower the activity of the complexes. Interestingly, **5**, **7**, and **8** are even two to three times more active than our previous coumarin-gold(I) complexes.[21]

Table 2: Determination of the IC50 values (µM) of complexes **4**-**8** by MTS assay at 48 h and comparison to their precursor N-methylimidazole, caffeine, ligand **1**-**3**, and to auranofin (values are presented as the mean ± SEM of at least three independent experiments with three replicates).

Compound	IC_{50} (µM)			
	MDA-MB-231	PC3	SW480	HEK293T
***N*-methyl benzimidazole**	> 100	> 100	> 100	> 100
caffeine	> 100	> 100	> 100	> 100
1	> 100	> 100	> 100	> 100
2	> 100	≈ 100*	> 100	≈ 75**
3	> 100	> 100	> 100	> 100
4	15 ± 3	15 ± 2	14 ± 2	5.0 ± 0.1
5	14 ± 2	16 ± 2	15 ± 2	5.2 ± 0.1
6	19 ± 3	15 ± 3	14 ± 3	5.2 ± 0.1
7	16 ± 2	17 ± 2	12 ± 3	4.9 ± 0.1
8	15 ± 2	16 ± 3	13 ± 1	4.9 ± 0.1
Auranofin	5.6 ± 0.1	9 ± 1	7.6 ± 1	1.7 ± 0.1

*viability at 100 µM ≈ 50% **viability at 75 µM ≈ 50%

***In vitro* imaging**

Coumarin derivatives are a class of fluorophores that displays a good brightness. Unfortunately, their maximal absorption wavelengths are too low for performing confocal microscopy of fluorescence experiments *in vitro* (under 350 nm, biological tissues absorb a lot the light). However, previously we noticed that sometimes coumarin derivatives can be good candidates for two photons microscopy.[21] Thus, we performed such experiments and we were able to image the different coumarin derivatives, even if photobleaching lowers the quality of image especially for **5**. All the coumarin derivatives enter the cells and present a homogeneous repartition in the cytoplasm. According to these images, the compounds do not seem to enter the nucleus or only weakly, which is in accordance with our previous studies and with the literature (DNA is not reported as one of the main target of gold(I) complexes).

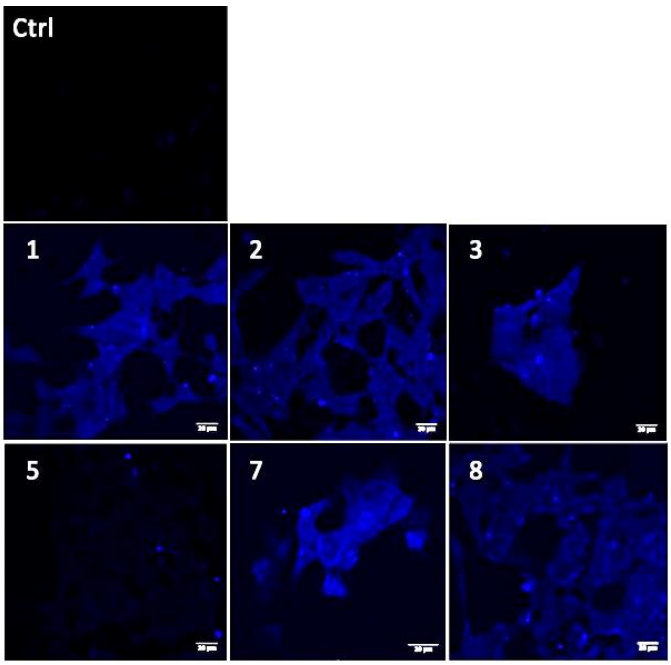

Figure 3: Biphoton images of the coumarine ligands (1, 2, 3, 5, 7 and 8) on human non-cancerous cell line HEK293T. Cells are incubated with 100µM of compound for 4h at 37°C, then fixed and permeabilized with iced MeOH and mounted with Fluoromount-G (Southern Biotech). Two-photon images are recorded upon 780 nm excitation (Chameleon IR laser from Coherent) and fluorescence emission collected through channel 1 ("DAPI channel") 400/492 nm.

Evaluation of anti-inflammatory effect

The anti-inflammatory effect of gold(I)-complexes **4**-**8** was evaluated on PBMC (Peripheral Blood Mononuclear Cells) a category of human leucocytes. These cells secrete pro-inflammatory cytokines such as Interleukine-1 beta (IL-1β) upon stimulation by LPS (LipoPolySaccharide), a bacterial wall component, during infections. As described for other compounds tested,[12,30,31] the performed tests consist in evaluation of the inhibition of produced-IL1-β by *in vitro* LPS-treated PBMC when they are also treated by variable concentration of the tested compounds. The anti-inflammatory response is validated when the production of IL1-β is partially or totally inhibited, while the viability of PBMC is superior to 60%.

The viability of PBMC is 63%, 61%, 77%, 77%, and 80% when incubated with the complexes **4**, **5**, **6**, **7**, or **8** respectively at a concentration of 1 µg/mL. Thus, the production of IL1-β was dosed at this concentration. Contrary to cytotoxicity, the complexes have different effects on inflammatory cytokine release. Indeed, **4** and **8** induce a strong inhibition of IL1-β production (98% and 74% respectively), **5** and **6** a non-significant one (20% and 5% respectively), while **7** induces an increase of 53% of IL1-β production. It is particularly interesting to notice that, unexpectedly, replacing methyl group borne by the imidazole ring by the coumarin moiety results in a higher level of IL1-β production (**4**→**5**: +78%; **6**→**7**: +58%). In these cases, the coumarin moiety did not improve the anti-inflammatory effect. On the contrary, when we change the position of the coumarin – complex **8** – it induces the opposite behaviour. It may suggest that steric hindrance on imidazole prevents the anti-inflammatory effect of gold moiety and even can induce a pro-inflammatory effect. A similar effect of the influence of slight moiety modification on inflammatory/anti-inflammatory effects was previously described for purine derivatives.[30]

These results indicate that compounds **4** and **8** are promising as anticancer and anti-inflammatory agents. Moreover, the good brightness of **8** should enable a future *in vitro* investigation of its biological mechanism of action.

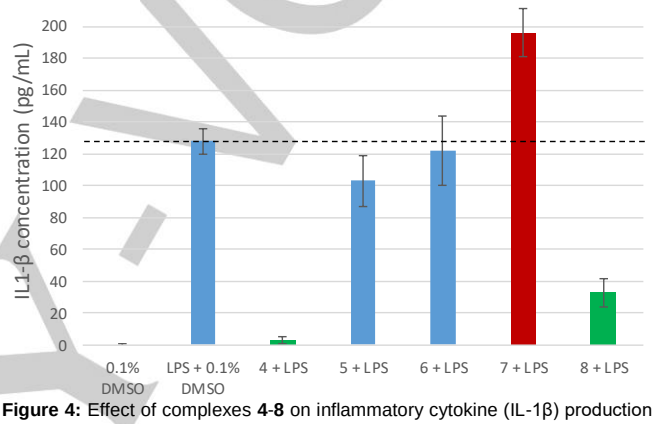

Figure 4: Effect of complexes **4**-**8** on inflammatory cytokine (IL-1β) production in LPS-stimulated PBMC vs a solution of DMSO (0.1%). All the compounds significantly below the black dashed line – in green – can be considered as anti-inflammatory agents, while the ones above it can be considered as pro-inflammatory agents (values are presented as the mean ± SEM of at least three independent experiments with three replicates).

Conclusions

We conceived a new family of cationic gold(I) trackable agents starting from benzimidazole or caffeine derivatives. All the complexes display high antiproliferative properties, while the ligands do not present significant toxicity. Coumarin derivatives have been imaged by two-photon microscopy, which indicates an accumulation of the compound in the cytoplasm. Interestingly, our study highlights the strong impact of the introduction of the coumarin moiety on the anti-inflammatory effect of the complex and, even more, the importance of its position on the caffeine scaffold. To finish, two complexes **4** and **8** seem to be very promising anticancer anti-inflammatory agents, which warrant further in depth investigation.

Experimental Section

General information

Otherwise specified, all reactions were carried out under Argon using conventional Schlenk techniques. CH_2Cl_2, and DMF were dried using an MBRAUN SPS 800 solvent purification system or distilled under

argon from appropriate drying agents and either used directly or stored under argon. The precursors [AuCl(tht)] and [AuCl(PPh_3)] have been synthesized according to literature procedures.[32,33] All other reagents were commercially available and used as received.

Synthesis part

See electronic supporting information for analytical data.

Compound **1**:
A round-bottom flask was charged with benzimidazole (1.2 eq., 105 mg, 0.892 mmol), 4 (bromomethyl)-7-methoxy-2H-chromen-2-one (1 eq., 200 mg, 0.743 mmol) and K_2CO_3 (2 eq., 205 mg, 1.486 mmol) in DMF (5 mL) under air. The reaction was stirred at room temperature overnight. After centrifugation and filtration through Celite®, the solvent was removed under vacuum by taking up three times in toluene (3 mL). After dissolution of the compound into dichloromethane (10 mL), the solution was washed twice with water (2 x 10 mL), then with a NaCl satured solution (10 mL). After drying over $MgSO_4$ and removal the solvent under vacuum, the product was obtained as an off yellow-brown powder (101 mg).

Compound **2**:
A round-bottom flask was charged with theophylline (1 eq., 100 mg, 0.555 mmol) and K_2CO_3 (2 eq., 153 mg, 1.110 mmol) in suspension into dry DMF (4mL)) under air. 4-(bromomethyl)-7-methoxy-2H-chromen-2-one (1.2 eq., 179 mg, 0.666 mmol) was added to the reaction mixture. The obtained white suspension was stirred at room temperature overnight. Water (2 V_{DMF}) was then added and the reaction mixture was cooled down in ice for 2 h. The formed yellow precipitate was collected by filtration, washed with 8 mL of water and precipitated in a dichloromethane/diethyl ether mixture. After drying under vacuum, the pure product was obtained as a yellow powder (91 mg).

Compound **3**:
A round-bottom flask was charged with theobromine (2 eq., 201 mg, 1.115 mmol), K_2CO_3 (4 eq., 308 mg, 2.230 mmol)) and 4-(bromomethyl)-7-methoxy-2H-chromen-2-one (1 eq., 150 mg, 0.557 mmol) in suspension into 5 mL of dry DMF. The suspension was stirred at 120°C overnight under air. Water (12 mL) was then added and the reaction mixture was cooled down in ice for 2h. The formed off-white precipitate was collected by filtration, washed with 5 mL of water and precipitated in a dichloromethane/diethyl ether mixture. After drying under vacuum, the pure product was obtained as an off-white powder (80 mg).

Compound **4**:
A Schlenk tube was charged with [AuCl(PPh_3)] (1 eq., 187 mg, 0.378 mmol) and $AgBF_4$ (1.1 eq., 81 mg, 0.416 mmol) in dichloromethane (13.5 mL). The solution was stirred for 30 min at room temperature in the dark. The obtained purple solution was filtered and transferred by cannula onto a solution of methylbenzimidazole (1 eq., 50 mg, 0.378 mmol) into methanol (2 mL). The mixture was stirred for 3 h at room temperature in the dark. After reaction, the solution was filtrated off through Celite®. The Celite was extracted with dichloromethane. Finally, the solvent was removed under vacuum to give a white product (161 mg).

Compound **5**:
A Schlenk tube was charged with [AuCl(PPh_3)] (1 eq., 81 mg, 0.163 mmol) and $AgBF_4$ (1.1 eq., 35 mg, 0.179 mmol) in dichloromethane (6 mL). The suspension was stirred for 30 min at room temperature in the dark. The resulting purple solution was filtrated and transferred by cannula onto a solution of 4-((1H-benzo[d]imidazol-1-yl)methyl)-7-methoxy-2H-chromen-2-one **1** (1 eq., 50 mg, 0.163 mmol) in dichloromethane (2 mL). The mixture was stirred for 3 h at room temperature in the dark. After centrifugation, the supernatant was isolated and the solvent was removed under vacuum to form a yellow product (124 mg).

Compound **6**:
A Schlenk tube was charged with [AuCl(PPh_3)] (1 eq., 178 mg, 0.361 mmol) and $AgBF_4$ (1.1 eq., 77 mg, 0.396 mmol) in dichloromethane (13 mL). The suspension was stirred for 30 min at room temperature in the dark. The obtained purple solution was filtered and transferred by cannula onto a solution of caffeine (1 eq., 70 mg, 0.361 mmol) into dichloromethane (2 mL). The mixture was stirred for 3 h at room temperature in the dark, then filtrated through Celite®. Finally, the solvent was removed under vacuum to form a white product (152 mg).

Compound **7**:
A Schlenk tube was charged with [AuCl(PPh_3)] (1 eq., 134 mg, 0.272 mmol) and $AgBF_4$ (1.1 eq., 58 mg, 0.299 mmol) in dichloromethane (6 mL). The suspension was stirred for 30 min at room temperature in the dark. The resulting purple solution was filtered and transferred by cannula onto a solution of 7-((7-methoxy-2-oxo-2H-chromen-4-yl)methyl)-1,3-dimethyl-1H-purine-2,6(3H,7H)-dione **2** (1 eq., 100 mg, 0.272 mmol) in dichloromethane (3 mL). The mixture was stirred for 3 h at room temperature in the dark then filtered through Celite®. The Celite® was rinced with dichloromethane (3 x 5 mL). The solvent was removed under vacuum to form a white product (123 mg).

Compound **8**:
A Schlenk tube was charged with [AuCl(PPh_3)] (1 eq., 100 mg, 0.202 mmol) and $AgBF_4$ (1.1 eq., 43 mg, 0.222 mmol) in dichloromethane (7.3 mL). The solution was stirred for 30 min at room temperature in the dark. The resulting purple solution was filtered and transferred by cannula onto a solution of 7-((7-methoxy-2-oxo-2H-chromen-4-yl)methyl)-3,7-dimethyl-1H-purine-2,6(3H,7H)-dione **3** (1 eq., 74 mg, 0.202 mmol) in dichloromethane (4 mL). The mixture was stirred for 3 h at room temperature in the dark. After centrifugation, the supernatant was isolated and the solvent was removed under vacuum to form a yellow product (138 mg).

Determination of antiproliferative activity in cancer cell line

MDA-MB-231, PC3, SW480 and HEK293T cells were purchased from American Type Culture Collection (ATCC, Manassas, VA). These cells were cultured in DMEM with 10% of foetal bovine serum and grown at 37°C in a humidified atmosphere containing 5% CO_2. Cells were seeded in 96-well flat-bottomed microplates (100 µL), cultured for 24 h before incubation with increasing concentrations of these compounds (from 1 to 175 µM) at 37°C for 48 h. Etoposide and 5-fluorouracil were used as anti-cancer references. Each treatment was performed in triplicate. The anti-cancer activity of compounds

and drug references were determined using the MTS assay (Promega®). This assay is based on the conversion of a tetrazolium compound [3-(4,5-dimethylthiazol-2-yl)-5-(3-carboxymethoxyphenyl)-2-(4-sulfo phenyl)-2H-tetrazolium, inner salt] in the presence of an electron coupling reagent (phenazine ethosulfate; PES) to formazan product by metabolically active cells. The amount of formazan produced was detected by measurement of the absorbance at 490 nm on a microplate reader ClarioStar. IC_{50} (*i.e.* the half maximal inhibitory concentration representing the concentration of a substance required for 50% *in vitro* inhibition) values were calculated using GraphPad7.0 Prism software.

In vitro two-photon microscopy experiments

Cells were seeded on chambered coverglass (24 well-plate) and allowed to recover. Cells were incubated with 100µM of each selected compounds at 37°C. After 4hrs cells were fixed and permeabilized with iced MeOH for 10 min at room temperature. Cells were then washed thrice with PBS (5min each) mounted with Fluoromount-G (Southern Biotech).

Biphoton imaging was performed using Nikon A1-MP multiphoton confocal microscope. Two-photon images are recorded upon 780 nm excitation (Chameleon IR laser from Coherent) and fluorescence emission collected through four detection channels, i.e., channel 1 ("DAPI channel") 400/492 nm, channel 2 ("FITC channel") 500/550, channel 3 ("Alexa channel") 563/588nm.

Determination of pro-inflammatory IL-1β cytokine production in PBMCs – (performed by Cohiro®)

Human peripheral blood mononuclear cells (PBMCs) were isolated from buffy coats from healthy donors by density gradient centrifugation (Pancoll human, d.1.077 g/mL). Recovered PBMCs were washed three times in Dulbecco's phosphate buffered saline, seeded in a 96-well microplate at $2x10^5$ cells/well in RPMI-1640 containing 10 % fetal bovine serum, penicillin (100 U/mL), streptomycin (100 µg/mL), amphotericin B (250 ng/mL), and incubated at 5 % CO_2 and 37°C. PBMCs were treated with compounds **4**, **5**, **6**, **7**, or **8** (1 µg/mL), then were stimulated for 24 h with 10 ng/mL of LPS (*E. coli*, 0128:B12, Sigma). Two anti-inflammatory references were tested in the same conditions: ZVAD (2.5 µg/mL → 75% of inhibition of IL-1β production) and dexamethasone (0.5 µg/mL → >99% of inhibition of IL-1β production). After incubation, the supernatants were harvested and kept at −20 °C until use. Viability of PBMCs was assessed by XTT assay. Secretion IL-1β was measured only in the culture supernatants of PBMCs treated with compounds that showed no or low toxicity, using a sandwich enzyme-linked immunosorbent assay (ELISA) method (eBioscience, San Diego, USA), according to manufacturer instructions.

X-Ray structure determinations and data

Compound **6**:
a single crystal of **6** was mounted in inert oil and transferred to the cold gas stream of a Bruker D8 VENTURE diffractometer. Crystal was kept at 100 K during data collection. Using Olex2,[34] the structure was solved with the XT[35] structure program using Intrinsic Phasing and refined with the XL[36] refinement package using Least Squares minimisation. The BF4- counter-anion was found disordered over two positions and refined using rigid group models with multiplicities converged to 0.52/0.48. Crystal Data for **6**: $C_{26}H_{25}AuBF_4N_4O_2P$ (M =740.24 g/mol): monoclinic, space group Cc (no. 9), a = 16.8252(7) Å, b = 7.2481(4) Å, c = 21.7429(11) Å, β = 93.597(2)°, V = 2646.3(2) Å^3, Z = 4, T = 100 K, μ(MoKα) = 5.680 mm^{-1}, Dcalc = 1.858 g/cm3, 63509 reflections measured (5.946° ≤ 2Θ ≤ 55.106°), 6032 unique (Rint = 0.0272, Rsigma = 0.0231) which were used in all calculations. The final R1 was 0.0113 (I > 2σ(I)) and wR2 was 0.0247 (all data). CCDC 1828665.

Compound **7**:
a single crystal of **7** was mounted in inert oil and transferred to the cold gas stream of a Bruker APEX II CCD diffractometer. Crystal was kept at 115 K during data collection. Using Olex2,[34] the structure was solved with the XT[35] structure program using Intrinsic Phasing and refined with the XL[36] refinement package using Least Squares minimisation. The diethyl ether solvate molecule was refined with a set of bond distance restraints (DFIX) as well as ADP restraints (RIGU). Crystal Data for **7**: $C_{40}H_{41}AuBF_4N_4O_6P$ (*M* =988.51 g/mol): triclinic, space group P-1 (no. 2), *a* = 12.4252(6) Å, *b* = 13.4076(6) Å, *c* = 13.7874(6) Å, *α* = 73.938(2)°, *β* = 68.552(2)°, *γ* = 69.165(2)°, *V* = 1969.43(16) Å^3, *Z* = 2, *T* = 115 K, μ(MoKα) = 3.847 mm^{-1}, *Dcalc* = 1.667 g/cm^3, 44313 reflections measured (5.592° ≤ 2Θ ≤ 55°), 9017 unique (R_{int} = 0.0451, R_{sigma} = 0.0379). CCDC 1828666.

Acknowledgements

Support was provided by the Conseil Régional de Bourgogne Franche-Comté, the Ministère de l'Enseignement Supérieur et de la Recherche, the Centre National de la Recherche Scientifique (CNRS), and the French Research National Agency (ANR) *via* project JCJC "SPID" ANR-16-CE07-0020, the Université de Bourgogne, the École Pratique des Hautes Études (EPHE). This work is part of the project PHARMACOIMAGERIE ET AGENTS THERANOSTIQUES and of the project CHIMIE DURABLE, ENVIRONNEMENT ET AGROALIMENTAIRE, supported by the Université de Bourgogne, Conseil Régional de Bourgogne through the plan d'actions régional pour l'innovation (PARI) and the European Union through the PO FEDER-FSE Bourgogne 2014/2020 programs. FrenchBIC is acknowledged for fruitful discussion. Anti-inflammatory tests have been performed by Cohiro® SAS. Dr M. Picquet, Dr Soustelle, and Ms M.-J. Penouilh are gratefully acknowledged for HR-MS, NMR and elemental analyses. Plateforme DimaCell, U. Bourgogne Franche-Comté, F21000 Dijon, France.

Keywords: theranostics • gold complex • bioinorganic chemistry • caffein • cancer

References:

[1] S. P. Pricker, *Gold Bull* **1996**, *29*, 53–60.
[2] C. F. Shaw, *Chem. Rev.* **1999**, *99*, 2589–2600.
[3] C. Roder, M. J. Thomson, *Drugs R D* **2015**, *15*, 13–20.
[4] T. M. Simon, D. H. Kunishima, G. J. Vibert, A. Lorber, *Cancer Res* **1981**, *41*, 94–97.

[5] https://clinicaltrials.gov/ct2/show/NCT01419691, **n.d.**
[6] L. M. Coussens, Z. Werb, *Nature* **2002**, *420*, 860–867.
[7] Z. Trávníček, P. Štarha, J. Vančo, T. Šilha, J. Hošek, P. Suchý, G. Pražanová, *J. Med. Chem.* **2012**, *55*, 4568–4579.
[8] J. Hošek, J. Vančo, P. Štarha, L. Paráková, Z. Trávníček, *PLOS ONE* **2013**, *8*, e82441.
[9] J. Vančo, J. Gáliková, J. Hošek, Z. Dvořák, L. Paráková, Z. Trávníček, *PLOS ONE* **2014**, *9*, e109901.
[10] R. Křikavová, J. Hošek, P. Suchý Jr., J. Vančo, Z. Trávníček, *Journal of Inorganic Biochemistry* **2014**, *134*, 92–99.
[11] B. Bertrand, P.-E. Doulain, C. Goze, E. Bodio, *Dalton Trans.* **2016**, *45*, 13005–13011.
[12] A. Trommenschlager, F. Chotard, B. Bertrand, S. Amor, L. Dondaine, M. Picquet, P. Richard, A. Bettaïeb, P. Le Gendre, C. Paul, et al., *Dalton Transactions* **2017**, *46*, 8051–8056.
[13] B. Bertrand, L. Stefan, M. Pirrotta, D. Monchaud, E. Bodio, P. Richard, P. Le Gendre, E. Warmerdam, M. H. de Jager, G. M. M. Groothuis, et al., *Inorg. Chem.* **2014**, *53*, 2296–2303.
[14] B. Bertrand, A. Citta, I. L. Franken, M. Picquet, A. Folda, V. Scalcon, M. P. Rigobello, P. L. Gendre, A. Casini, E. Bodio, *J Biol Inorg Chem* **2015**, *20*, 1005–1020.
[15] B. Bertrand, E. Bodio, P. Richard, M. Picquet, P. Le Gendre, A. Casini, *Journal of Organometallic Chemistry* **2015**, *775*, 124–129.
[16] B. Bertrand, A. de Almeida, E. P. M. van der Burgt, M. Picquet, A. Citta, A. Folda, M. P. Rigobello, P. Le Gendre, E. Bodio, A. Casini, *Eur. J. Inorg. Chem.* **2014**, *2014*, 4532–4536.
[17] B. Bertrand, A. de Almeida, E. P. M. van der Burgt, A. Citta, A. Folda, E. Bodio, M. Picquet, M. P. Rigobello, P. Le Gendre, A. Casini, *J. Biol. Inorg. Chem.* **2014**, *19*, S792–S792.
[18] L. Stefan, B. Bertrand, P. Richard, P. Le Gendre, F. Denat, M. Picquet, D. Monchaud, *ChemBioChem* **2012**, *13*, 1905–1912.
[19] B. Bertrand, K. Passador, C. Goze, F. Denat, E. Bodio, M. Salmain, *Coordination Chemistry Reviews* **2018**, *358*, 108–124.
[20] L. Dondaine, D. Escudero, M. Ali, P. Richard, F. Denat, A. Bettaieb, P. Le Gendre, C. Paul, D. Jacquemin, C. Goze, et al., *Eur. J. Inorg. Chem.* **2016**, *2016*, 545–553.
[21] M. Ali, L. Dondaine, A. Adolle, C. Sampaio, F. Chotard, P. Richard, F. Denat, A. Bettaieb, P. Le Gendre, V. Laurens, et al., *J. Med. Chem.* **2015**, *58*, 4521–4528.
[22] J. M. Madar, L. A. Shastri, S. L. Shastri, M. Holiyachi, N. Naik, R. Kulkarni, F. Shaikh, V. Sungar, *Synthetic Communications* **2018**, *48*, 375–386.
[23] M. Holiyachi, S. Samundeeswari, B. M. Chougala, N. S. Naik, J. Madar, L. A. Shastri, S. D. Joshi, S. R. Dixit, S. Dodamani, S. Jalalpure, et al., *Monatsh Chem* **2018**, 1–15.
[24] A. Samala, K. G, S. K. Bagh, *Der Pharma Chemica* **2016**, *8*, 19–24.
[25] Y. A. Selim, N. H. Ouf, *Organic and Medicinal Chemistry Letters* **2012**, *2*, 1.
[26] S. N. Mangasuli, K. M. Hosamani, H. C. Devarajegowda, M. M. Kurjogi, S. D. Joshi, *European Journal of Medicinal Chemistry* **2018**, *146*, 747–756.
[27] A. M. Brouwer, *Pure and Applied Chemistry* **2011**, *83*, DOI 10.1351/PAC-REP-10-09-31.
[28] P.-E. Doulain, R. Decréau, C. Racoeur, V. Goncalves, L. Dubrez, A. Bettaieb, P. L. Gendre, F. Denat, C. Paul, C. Goze, et al., *Dalton Trans.* **2015**, *44*, 4874–4883.
[29] S. Tasan, O. Zava, B. Bertrand, C. Bernhard, C. Goze, M. Picquet, P. Le Gendre, P. Harvey, F. Denat, A. Casini, et al., *Dalton Trans.* **2013**, *42*, 6102–6109.
[30] L. Maugé, T. Fotopoulou, S. Delemasure, P. Dutartre, M. Koufaki, J.-L. Connat, *Eur. J. Pharmacol.* **2014**, *730*, 148–156.
[31] L. Teyssier, J. Colussi, S. Delemasure, J. Chluba, D. Wendehenne, O. Lamotte, J.-L. Connat, *Frontiers in Public Health* **2017**, *5*, DOI 10.3389/fpubh.2017.00074.
[32] R. Uson, A. Laguna, M. Laguna, D. A. Briggs, H. H. Murray, J. P. Fackler, in *Inorganic Syntheses* (Ed.: H.D. Kaesz), John Wiley & Sons, Inc., **1989**, pp. 85–91.
[33] N. Mézailles, L. Ricard, F. Gagosz, *Org. Lett.* **2005**, *7*, 4133–4136.
[34] O. V. Dolomanov, L. J. Bourhis, R. J. Gildea, J. A. K. Howard, H. Puschmann, *Journal of Applied Crystallography* **2009**, *42*, 339–341.
[35] G. M. Sheldrick, *Acta Crystallographica Section C Structural Chemistry* **2015**, *71*, 3–8.
[36] G. M. Sheldrick, *Acta Crystallographica Section A Foundations of Crystallography* **2008**, *64*, 112–122.

Entry for the Table of Contents

Insert graphic for Table of Contents here. ((Please ensure your graphic is in **one** of following formats))

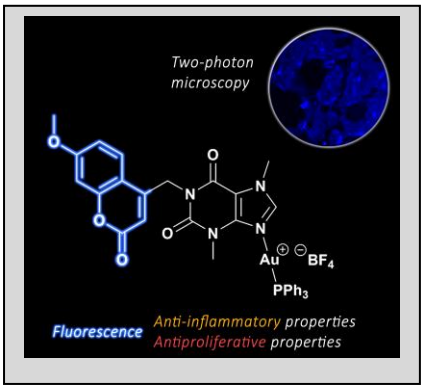

Au(I)-caffeine-based therapeutic agents displaying both antiproliferative and anti-inflammatory properties have been synthesized, characterized, and tracked *in vitro* by two-photon microscopy. The impact of the position of the coumarin probe on biological properties have been highlighted.